

Continuous strain measurements in a shotcrete tunnel lining using distributed fibre optic sensing

Christoph M. Monsberger¹, Werner Lienhart¹, Alexander Kluckner²,
Lukas Wagner² and Wulf Schubert²

¹ Institute of Engineering Geodesy and Measurement Systems, Graz University of Technology, Austria, christoph.monsberger@tugraz.at

² Institute of Rock Mechanics and Tunnelling, Graz University of Technology, Austria

Abstract

In modern tunnelling, deformation monitoring is an important component to ensure a safe construction and a long lifetime of the tunnel. It is state of the art to measure displacements at the surface of the tunnel lining using total stations or terrestrial laser scanners and internal deformations with electric strain gauges. However, these measurements do not deliver a complete picture of the utilization within the lining and new methods must be evolved.

In this paper, the authors report about the design and realization of a distributed fibre optic sensing system for conventional tunnelling, which was installed in the shotcrete lining in the core of a fault zone at a railway tunnel under construction. Therefore, sensor cables in various layers for distributed strain and temperature sensing with a total length of more than 230 m were placed in the cross-section of the tunnel. Due to the high spatial resolution of the system, thousands of measurement points could be realized and completely new information about the strain distribution in the lining could be gathered. Autonomous monitoring was started immediately after the installation and measurements were performed during the curing of the shotcrete as well as during the advance of the tunnel drive over several weeks. In order to prove the suitability of the fibre optic system, the results were compared to internal strain measurements of vibrating wire sensors and also to strains derived from geodetic measurements.

In addition to the field measurements, the performance of the sensing system and its robustness were investigated with a load test of a concrete beam structure. These results in combination with the outcomes of the continuous monitoring campaign demonstrate the high potential of distributed fibre optic sensing systems and their capability to extend classical measurement methods in tunnelling.

1. Introduction

To ensure structural stability is one of the major tasks in tunnelling. For that reason, geotechnical monitoring systems and reliable data interpretation are essential in order to assess and improve the geological underground model for a safe construction and operation. It is state of the art to mount geodetic target points to the surface of the tunnel lining and to measure displacements using total stations (1). However, these measurements do not provide information about the internal strain distribution and readings are usually taken only once per day. Hence, the strain development cannot be recorded continuously with an adequate temporal resolution. In geological fault zones,

strain gauges, e.g. vibrating wire sensors (VWS), may be additionally to measure the strain behaviour inside the shotcrete lining and to determine the degree of utilization. Although continuous measurements can be performed using this technique, each electrical sensor needs its own connecting cable. Therefore, the number of sensors that can be attached to one lining is limited due to practical reasons and the gained data only provides information at specific points.

Distributed fibre optic sensing (DFOS) systems are advantageous compared to electrical sensors, as there is only one lead-in cable necessary to realize thousands of measurement points. Thus, the installation effort can be massively reduced and the strain distribution can be gathered with a suitable spatial resolution. However, since an optical glass fibre acts as the sensing element, robust sensing cables are required and tailored installation techniques must be developed to protect the sensor during construction and monitoring of the tunnel lining. Based on this fact, only a few specific distributed fibre optic monitoring approaches in conventional tunnelling are known, in which mostly Brillouin analysers with a typical spatial resolution of 0.5 m to 1 m were used, see e.g. (2).

This paper reports about the design and realization of a distributed fibre optic measurement system for conventional tunnelling based on Rayleigh backscattering. The high spatial resolution of the system of up to 10 mm enables the identification of local damages or failure zones, which might not be detected by distributed Brillouin sensors. In the following, the components of the fibre optic system are described (Sec. 2.1 and 2.2) and the relevance of calibration is discussed (Sec. 2.3). Furthermore, laboratory investigations of a concrete beam structure are presented (Sec. 3), in which the robustness of the sensing cables and the performance of the entire sensing system were assessed. Afterwards, the installation of the system inside the shotcrete lining of a railway tunnel under construction is introduced (Sec. 4.1) and results of an autonomous monitoring campaign over several weeks are depicted (Sec. 4.2). Finally, the suitability of the system for conventional tunnelling is discussed and an outlook on future research is given (Sec. 5).

2. Fibre optic measurement system

As a result of the advantages already mentioned above, various novel applications for DFOS systems in civil engineering and especially in geotechnical applications are realized in recent years, see e.g. (3) or (4). All of them have shown that the interaction of several components of the fibre optic system is highly relevant to provide a suitable field monitoring system. In this section, the capabilities of the interrogation unit and the structure of the installed strain sensing cable type are introduced. In addition, the basic sensing principle and the significance of a reliable system calibration are presented.

2.1 Optical backscatter reflectometer (OBR)

Rayleigh scattering causes about 85% of the natural attenuations in optical fibres (5) and is one of the major effects of intensity loss along the fibre core. Considering the backscattered signal, the amplitude has a random but static behaviour. External influences, like changes in strain or temperature, result in a frequency shift between two measurements in the locally reflected Rayleigh pattern. The influencing quantities are determined by observing a small fibre segment in the frequency domain, which can be

interpreted as a weak reflecting fibre Bragg grating (FBG) with a random period. Finally, the distributed sensing system is realized by splitting the fibre in equidistant segments (equivalent to the spatial resolution) and calibrating the local Rayleigh shift in reference to changes in strain or temperature.

For strain monitoring at the tunnelling project presented in this publication, an optical backscatter reflectometer (OBR) from Luna Innovations Inc. (see Fig. 1a) was used. Based on the so-called optical frequency domain reflectometry (OFDR) technique, this interrogation unit is able to record sensing information with a very high resolution of about $1.0 \mu\epsilon$ (respectively $1 \mu\text{m/m}$) for strain and about 0.1 K for temperature measurements (6). Moreover, a high spatial resolution of about 10 millimetres or even better can be achieved. Further information about the determination principle may be found in (3). For details on the optical network of the system, see e.g. (7).

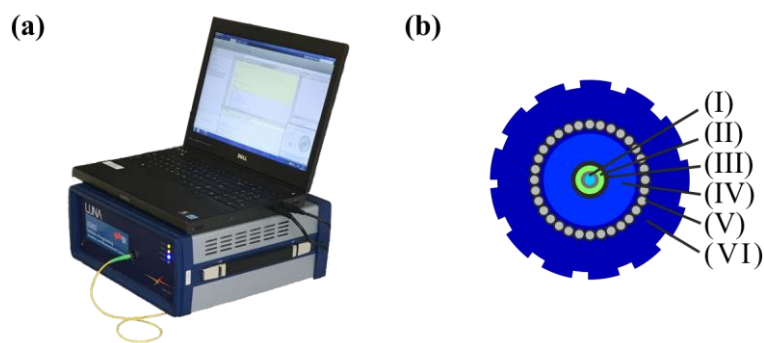


Figure 1. Fibre optic measurement system: (a) Luna Technologies Inc. OBR 4600 and (b) structure of strain sensing cable BRUsens V3 from Brugg Cables AG with (I) strain sensing single mode fibre ($\varnothing 250 \mu\text{m}$), (II) multi-layer buffer with strain transfer layer, (III) metal tube, (IV) polyamide inner protection layer, (V) special steel armouring and (VI) structured polyamide outer sheath

2.2 Strain sensing cable

In civil engineering, optical fibres usually have to withstand harsh environmental conditions at the construction site. For that reason, robust sensing cables are necessary to protect the fibre during the field installation and monitoring. However, an unbiased strain transfer from the outer sheath to the sensitive fibre core is highly relevant for strain sensing applications, why all cable layers must be reliably interlocking.

For fibre optic strain measurements in geotechnical projects, Brugg Cables AG offers various types of strain sensing cables. Fig. 1b depicts the basic structure of the sensing cable BRUsens V3 (8), which was selected for the monitoring in the presented applications. This cable with a diameter of about 7 mm protects the optical fibre (I) with a special metal tube (III) and an interlocking multi-layer buffer (II) ensures a reliable strain transfer. The outer protection consists of an inner polyamide layer (IV), a special steel armouring (V) and a polyamide outer sheath (VI), whereby the structured surface guarantees a solid bond with the surrounding material.

The protection layers make the cable more robust against mechanical impacts, but it has to be considered that the flexibility (minimal bending radius, etc.) is limited due to these additional layers. Even if this drawback must be accepted inside the tunnel to guarantee the integrity of the sensing fibre, more flexible cable types might fit better in other civil engineering applications. As this paper shows only a small selection of sensing cables, reference is given to (3).

2.3 Principle of system calibration

As mentioned in Sec. 2.1, the raw OBR measurement is the local Rayleigh frequency shift between a reference scan and subsequent measurements, from which strain and temperature changes can be determined. This transfer requires individual calibration parameters for each sensing cable type. However, many manufactures of fibre optic sensors refer to literature values without further notice, which might result in errors up to 10% (9). For that reason, the Institute of Engineering Geodesy and Measurement Systems (IGMS) developed a unique calibration device within the last years. Key components of this facility are the stable setup on a 30 m concrete bench, a linear translation stage that allows sensor elongations up to 300 mm and a laser interferometer that is used for a precise reference measurement (10).

In order to calibrate the fibre optic system, the transfer from the measured wavelength shift $\Delta\lambda$ [nm] or the frequency shift $\Delta\nu$ [GHz] to the sensing quantities strain ε and temperature changes ΔT can be approximated by the linear function

$$\frac{\Delta\lambda}{\lambda} = \frac{-\Delta\nu}{\nu} = K_\varepsilon \varepsilon + K_T \Delta T \quad (1)$$

with the normalized sensitivity coefficients K_ε and K_T and the centre wavelength λ or centre frequency ν of the measurement. As the calibration facility is set up in the IGMS temperature and humidity controlled laboratory, the temperature is constant and the measurement signal only depends on strain:

$$\frac{\Delta\lambda}{\lambda} = \frac{-\Delta\nu}{\nu} = K_\varepsilon \varepsilon \quad \left|_{\Delta T = \text{const.}} \quad (2)$$

Prior to field installations, IGMS usually performs an individual strain calibration of a sample of each used sensing cable on the calibration facility to avoid systematic errors within the data acquisition on site. These investigations have shown that the estimated strain sensitivity coefficients K_ε of different strain sensing cables from Brugg Cables AG vary in a range between 0.748 and 0.786. Although these values basically agree to specifications from literature, see e.g. (7), the resulting strain values might depict errors up to 5% for each sensing cable type without an individual calibration. Based on that fact, the individual determination of K_ε has to be considered as a very important part in the development of a reliable fibre optic sensing system. Further information on strain calibration of sensing cables for geotechnical applications may be found in (3).

In real world applications, especially in long-term monitoring, raising temperature effects must be eliminated to provide unaffected strain values of the monitored object. For that, an unstrained fibre can be installed nearby the strain sensing cable for temperature compensation. Another solution is to utilize an additional distributed fibre optic sensing system based on Raman scattering for temperature measurements along the strain sensing cable. This technology is basically independent from strain and can therefore be used for temperature compensation too, see e.g. (11).

3. Laboratory tests

In order to assess the robustness of the fibre optic sensing cable and the performance of the entire DFOS system, a concrete beam test structure was instrumented and investigated under controlled load at Graz University of Technology. In the following, the instrumentation as well as the test setup is presented, selected OBR measurements are discussed and compared to results of a Brillouin analyser system.

3.1 Production and fibre optic instrumentation

Similar to a typical shotcrete lining in conventional tunnelling, the test structure with a total length of 6 m was manufactured with two reinforcement layers, see Fig. 2. To evaluate the distributed evolution of strain, different types of sensing cables for strain measurements and temperature compensation were mounted along the upper and lower longitudinal reinforcement using cable ties. After concreting, the structured surface of the strain sensing cables forms a solid bond with the surrounding material and a reliable strain transfer to the optical fibre can be ensured. Fibres for temperature compensation were loosely installed inside a tube and should therefore not be affected by mechanical strain.



Figure 2. Production of concrete beam structure

In addition to DFOS cables, FBG sensors inside the structure as well as conventional electrical sensors at the surface were also installed. As this paper is focussed on distributed fibre optic sensing, measurement results of other sensing techniques and further information about the testing concept may be found in (12).

The instrumented concrete beam structure was investigated in a 4-point loading test 29 days after concreting. The test setup was split up into two different phases (see Fig. 3). In state S-01, a normal load of 1600 kN was initially applied, which significantly increases the theoretical elastic limit of the structure up to a vertical load of 175 kN. All applied vertical loads were below this elastic limit and therefore, only elastic deformation during this phase can be expected. At the beginning of state S-02, the normal load was totally released, which results in a significant decrease of the elastic vertical load limit to about 50 kN. The structure was stepwise loaded vertically until the lower reinforcement layer failed, which happened after load step #13 during increasing the load up to 150 kN.

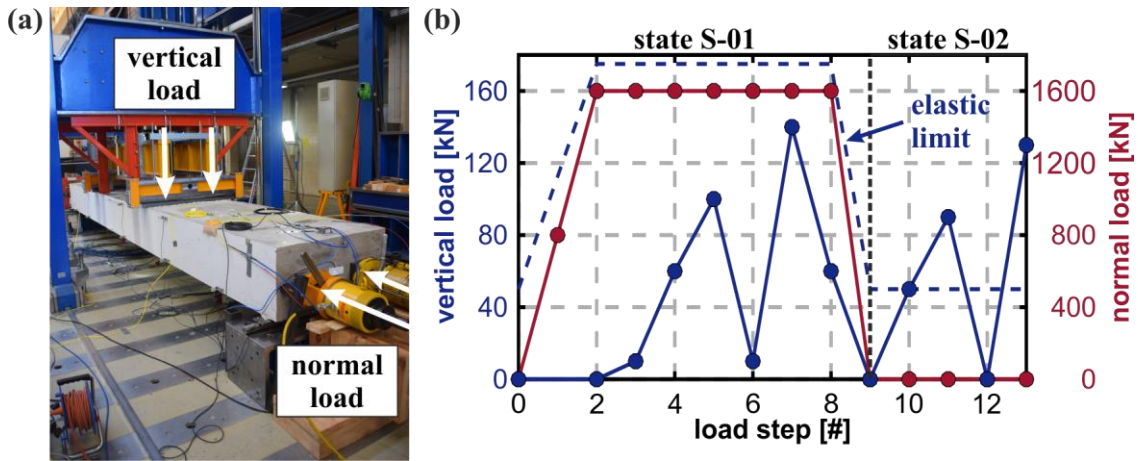


Figure 3. Loading test setup: (a) Instrumented concrete beam mounted in testing facility and (b) applied test loads

3.2 Measurement results

The distributed strain profiles measured by the OBR at each vertical load step of state S-01 after applying the normal load are displayed in Fig. 4a. It can be seen that only negative strain values (contraction) arise along the lower longitudinal reinforcement. As a result of the high normal load, the contraction outweighs the elongation due to the bending of the beam.

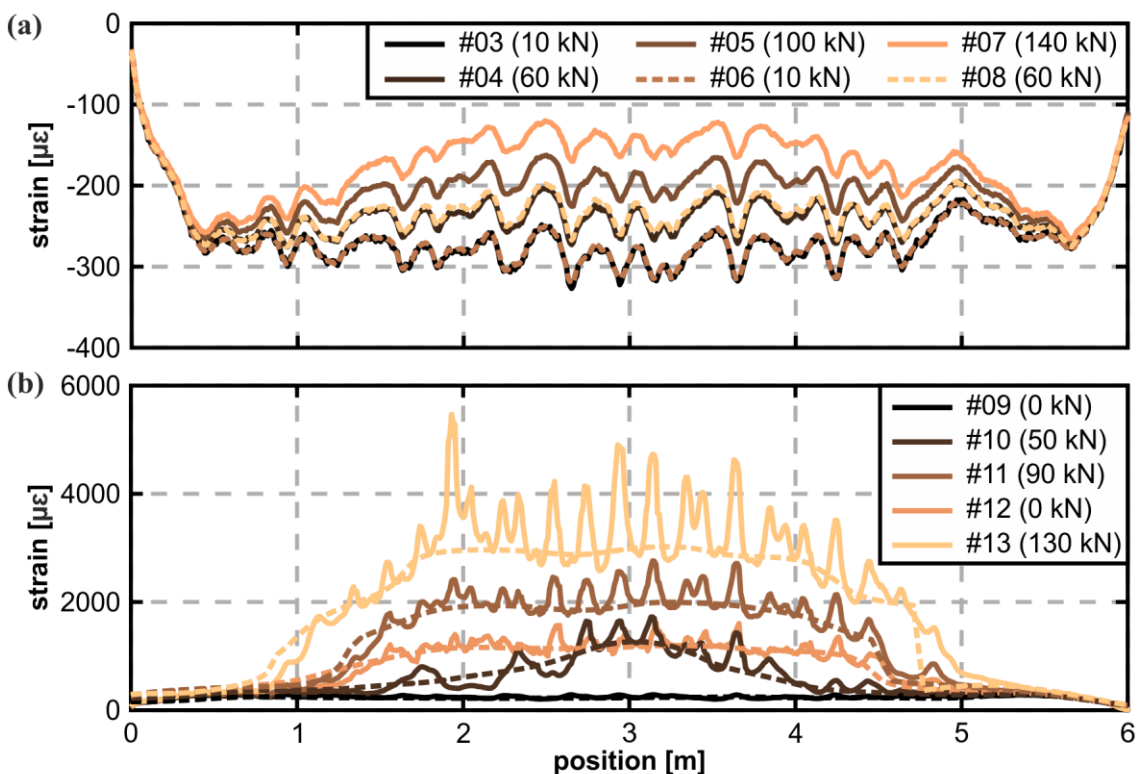


Figure 4. Distributed fibre optic strain profiles along the lower longitudinal reinforcement: (a) State S-01 measured by the OBR and (b) state S-02 measured by the OBR (solid lines) and Brillouin sensing unit (dotted lines); ordinate: negative values = contraction, positive values = elongation; values in the parentheses in the legends correspond to the applied vertical load

Although all different load steps can be clearly identified and related to the applied vertical load, a slight inhomogeneous strain pattern with a maximum amplitude of about $35 \mu\epsilon$ becomes visible along the profiles. Possible reasons for these effects might be inhomogeneities in the concrete structure, a slight non-uniform bond between the sensing fibre and the surrounding concrete material or an interaction between the different protection layers of the sensing cable. However, the evolving pattern seems to be constant after applying the normal load and therefore, the strain profiles show a perfect repeatability before and after loading (e.g. #03 and #06) with strain deviations in the range of only a few $\mu\epsilon$. This conformity also proves the fact that only loadings within the elastic limit were applied to the concrete structure the first test state.

Starting state S-02, both the normal load and the vertical load were totally released. Therefore, the strain profiles measured by the OBR in Fig. 4b depict only slight variations at the first load step (#09) resulting from the arising strain pattern of the state S-01. After increasing the load to 50 kN (#10), local strain peaks become visible along the strain profile. These inhomogeneities can be related to cracks in the concrete, which start to evolve at this load step. In the following, the vertical load was further increased up to 90 kN and reduced to zero afterwards. Although the structure is free of any external load at load step #12, positive strain is recorded at the lower reinforcement layer. It seems that the structure has already plastically deformed at this load step and thus, irreversible strain remain. At the last recorded load step (#13), strain peaks are visible at positions between 1.0 m and 5.0 m, which can be related to cracks and are in good agreement to manual tape measurements at the surface.

In addition to the high-resolution OBR system (Fig. 4b, solid lines), the sensing fibres were also interrogated using a Brillouin sensing unit FT2505 from fibrisTerre Systems GmbH (Fig. 4b, dotted lines). The results of both technologies depict a similar behaviour. However, it can be seen that the cracks cannot be identified with the used Brillouin analyser due to the low spatial resolution of 0.5 m.

4. Field measurements

As part of a research project in cooperation with the Austrian Federal Railways (ÖBB-Infrastruktur AG), the developed fibre optic system was installed in the shotcrete lining close to the tunnel face of a tunnel drive of the Semmering Base Tunnel, Austria. (13) Subsequently, the installation setup is shortly introduced and fibre optic measurement results as well as comparisons to other conventional sensing techniques are presented.

4.1 Monitoring concept and sensor installation

Based on the New Austrian Tunnelling Method (NATM), conventional tunnelling is usually performed in excavation sequences, which enables the rock to support itself (14). The construction of the tunnel section, in which the fibre optic system was installed in one cross-section, can be divided into two essential parts: First, the top-heading area is excavated and supported by bolts, lattice girders and a reinforced shotcrete lining. The drive and support of the top-heading continues for several meters depending on geological conditions. Then, the bench/invert area is excavated and supported by reinforced shotcrete to form a load-bearing ring system.

As schematically depicted in Fig. 2a, two different layers of fibre optic sensing cables were placed at the outer (rock-side) as well as the inner (cavity-side) reinforcement

layers at the top-heading and bench/invert to provide distributed measurements along the entire cross-section. The first sensing layer was placed in peripheral direction perpendicular to the tunnel axis (red). The other one is guided in a loop configuration alternately parallel and perpendicular to the tunnel axis (yellow) to measure the occurring strain in different distances as well as different orientations to the tunnel face. An additional BRUsens V3 cable was loosely installed in a cladding tube nearby the strain sensing cables in peripheral direction for temperature compensation. Since the distance between the different strain sensing layers is less than one metre, it was assumed that this arrangement is sufficient enough to compensate occurring temperature effects reliably.

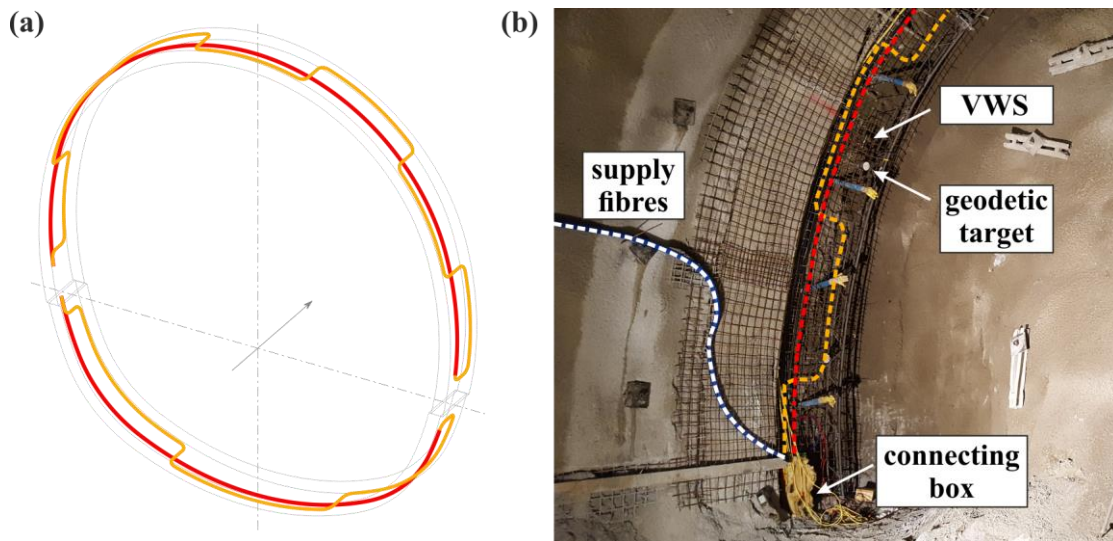


Figure 5. Installation of fibre optic sensing system inside the tunnel lining: (a) Schematic representation and (b) practical realization

The optical connectors of all sensing cables were assembled in a connecting box directly installed in the monitoring section under investigation, from where supply fibres were used to connect the sensing cables to the measurement unit. The OBR itself was placed about 60 m behind the instrumented cross-section in a specially manufactured measurement box. To verify the measurement results of the DFOS system, also conventional geodetic bi-reflex targets and vibrating wire strain (VWS) gauges were installed at the cross-section, see Fig. 5b.

4.2 Continuous monitoring and measurement results

In order to obtain a complete picture of the deformation of the shotcrete liner from the very beginning, continuous monitoring of each instrumented lining segment was started right after shotcrete application using the OBR in combination with an own IGMS-developed measurement software. All cable layers were measured sequentially with a sampling rate of about 1 minute. The resulting strain values represent the changes in strain to the first measurement, the so-called reference measurement.

Fig. 6 depicts the strain distribution along the fibre sensing layer at the rock-side layer of wire mesh in peripheral direction at selected times. First compression zones at the crown and the shoulders (top-left, top-right) are already visible 12 hours after construction of top-heading (Fig. 6a). The maximum deformation is observed at the left

shoulder, where also the largest displacement values were obtained by the conventional geodetic measurements over the monitoring period (13). However, the DFOS system enables an exact localization of the maximum (absolute) strain within the cross-section instantly. About 48 hours after the construction (Fig. 6b), the compression zones have increased further and no more tension zones are visible along the entire cross-section. It has to be noted that the deformation of the liner results from the deformation of the rock mass as well as deformations due to shotcrete specific characteristics (shrinkage, creep).

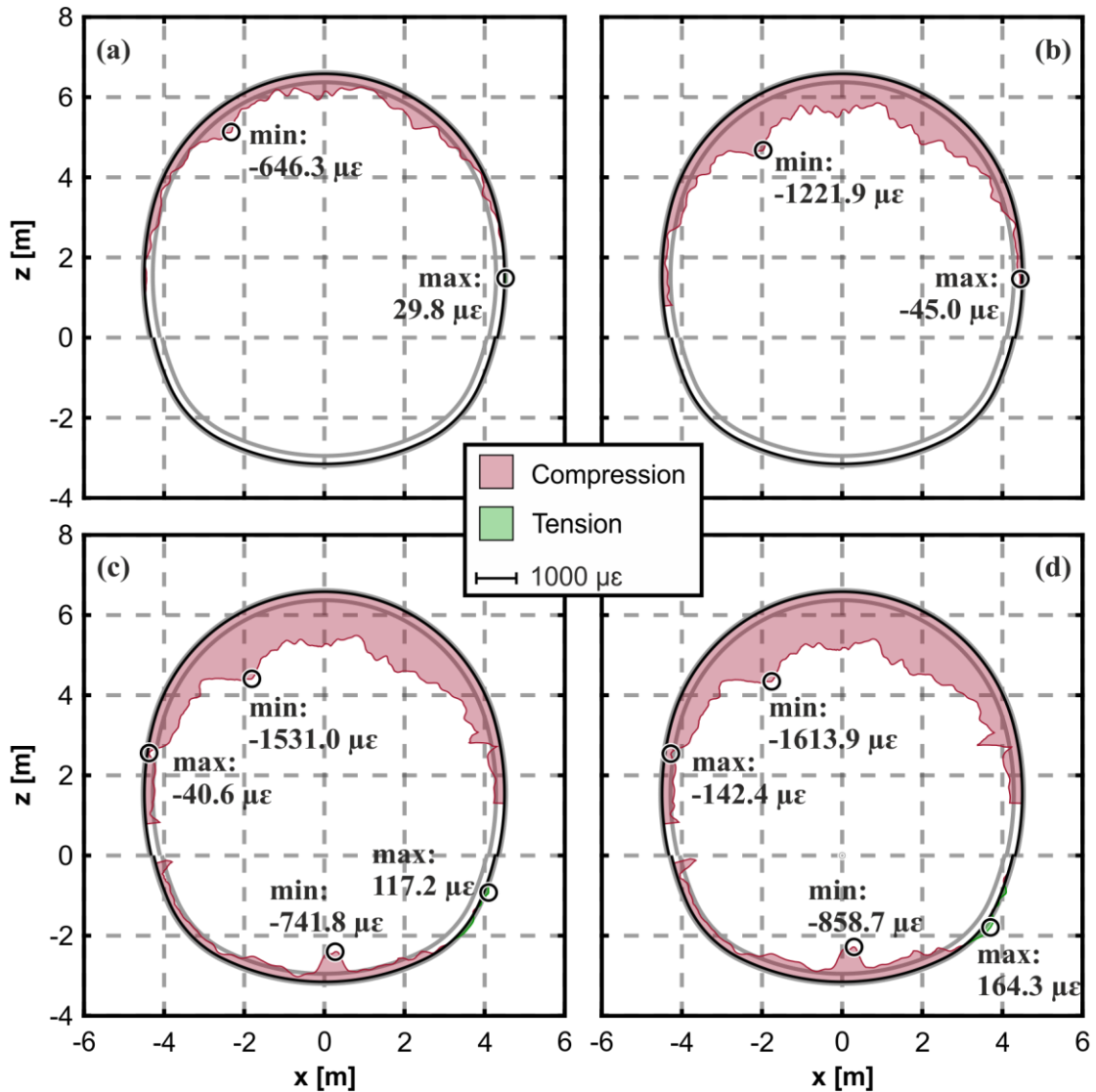


Figure 6. Measured strain distribution at the rock-side layer in peripheral direction: (a) 12 hours after installation at top-heading, (b) 48 hours after installation at top-heading, (c) 12 hours after installation at invert and (d) 48 hours after installation at invert

The construction of the bench/invert was performed about five days after the top-heading area. Immediately after the installation (Fig. 6c), the strain profiles at the rock-side reinforcement layer in the liner of the bench/invert section depict slight compression as well as tension zones and one local strain peak at the invert point, which might be a result of overlaying reinforcement layers or distortions through other sensors in this area. In the meantime, also compressional strain increased significantly at the

top-heading. About 48 hours after the construction of the bench/invert (Fig. 6d), the deformation progress along the cross section is still ongoing, but seems to be almost constant along the entire ring. This suggests that the installed supporting ring forms a load-bearing system, which is capable to cope with the remaining loads.

In order to compare the fibre optic results to the vibrating wire sensor measurements (see Fig. 7a), the strain values in the area of the VWS are averaged. Although the different sensors are not exactly located at the same position inside the lining (meaning in direction of the drive), the measurements show a good agreement in shape as well as in magnitude. Conventional geodetic measurements usually deliver 3D displacements. However, length changes of the chord between two neighbouring bi-reflex targets can be derived from the 3D displacements. These may be interpreted as strains of the entire chord and can therefore be compared to the average strain of the DFOS measurements in the same area. For better data interpretation, the standard deviation of the derived strain values can also be determined by assuming an average measurement precision of the 3D target (here: 1 mm). The resulting time series of one selected chord length in Fig. 7b basically depict a similar behaviour, but deviations of about $250 \mu\epsilon$ arise over time. Even if the deviations are more or less within the range of the standard deviation (1σ) of the derivation principle, this effect seems to be systematic.

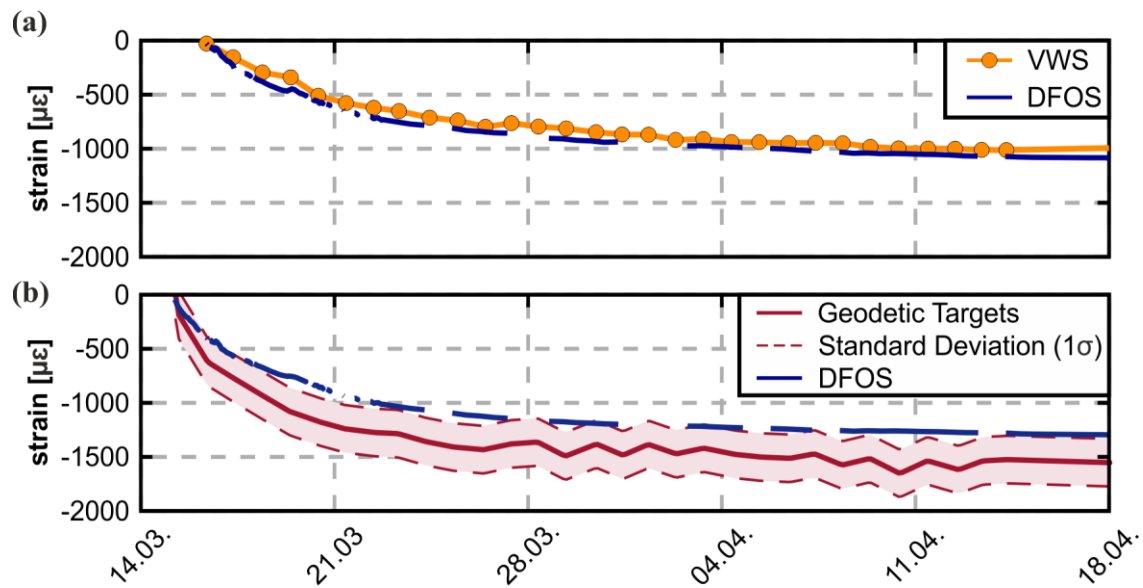


Figure 7. Comparison of fibre optic results to conventional monitoring techniques: (a) Vibrating wire sensors and (b) strains derived from classical geodetic measurements

Considering the sensor arrangement in Fig. 5b, it becomes obvious that the geodetic target points are mounted closer to the tunnel face than the DFOS cables in peripheral direction, which might explain the aforementioned deviations. To evaluate the influence of the sensor position with respect to the position of the tunnel face of the current excavation round, the distributed strain profiles of the sensing cable in loop configuration (see Fig. 4a) before and after the excavation of the next round are plotted in Fig. 8. The results show that higher compressional strains arise immediately after the excavation at positions, where the sensing cable is mounted closer to the tunnel face. This effect is especially visible in the area next to the crown. About 6 hours later, compressions at these areas (#02 and #03 in Fig. 8b) are about $700 \mu\epsilon$ higher than at the crown area, which is about 65 cm far off the tunnel face of the first excavation round.

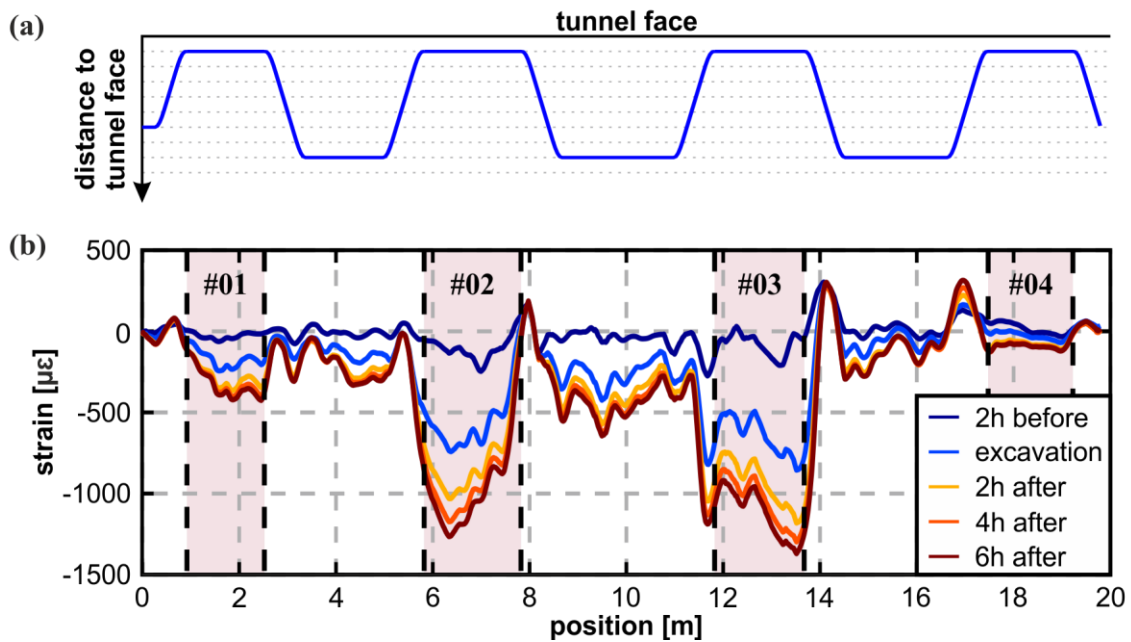


Figure 8. Fibre optic measurements along the top-heading section in different distances to tunnel face: (a) Position of sensing cable relative to tunnel face and (b) distributed strain profiles

In order to analyse this relation over the entire monitoring period, the strain values along each section (#01 to #04) can be averaged and compared to results of the sensing fibre installed in peripheral direction in the same area. Simply put, the average strain values of different sections along the top-heading in peripheral direction with different distances to the tunnel face are plotted in Fig. 9. It can be seen that deviations between strain recorded at the different sensor positions arise shortly after the installation (and further excavation), but remain constant after some time. The effect is much larger, but not limited to the crown area, where differences of about $700 \mu\epsilon$ can be observed. Even at the side walls, deviations up to $380 \mu\epsilon$ occur over time. From this, it can be concluded that the position of the sensor with respect to the position of the tunnel face has a major influence on the strain development and must be considered for data interpretation and for comparison of recordings of different sensing techniques.

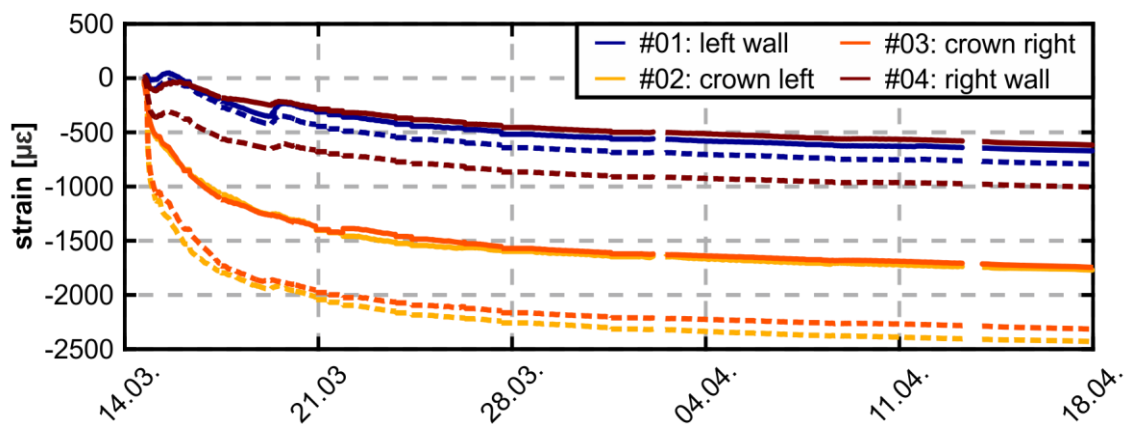


Figure 9. Average strain values at different positions (#01 to #04) along the instrumented cross-section in a distance of 10 cm (dotted lines) and 75 cm (solid lines) to the tunnel face of the first round

5. Conclusions

This paper reported about a DFOS system based on Rayleigh backscattering to monitor distributed strains in a shotcrete lining of a conventionally driven tunnel with high spatial resolution. For this, reliable fibre optic components had to be found, which can withstand the harsh environments inside the tunnel. In order to assess the robustness of the fibre optic sensing cable and the performance of the system, laboratory investigations were carried out, for which a concrete beam structure was instrumented and investigated in a 4-point loading test. The investigations have shown that the selected sensing cables are sufficiently robust to ensure the integrity of the optical fibre during concreting and monitoring. In the test, the used interrogation unit was able to record the strain distribution along the embedded sensing cables and also to capture local strain events like cracks inside the structure.

The developed fibre optic system was installed in the shotcrete lining at a monitoring section of a railway tunnel currently under construction and novel information could be gathered. The distributed sensing approach enables an exact localization of maximum strain within the cross section and the deformation history can be recorded continuously along the entire section. Moreover, it could be shown that the position of the sensor in the direction of the tunnel drive within the monitoring section significantly determines the strain recordings.

The installed system was designed to allow follow-up measurements after the initial continuous monitoring campaign. Hence, future research will focus on the long-term monitoring of the instrumented cross-section to assess the further deformation progress inside the shotcrete lining. This will finally lead to a better understanding of the strain distribution of shotcrete linings at conventionally driven tunnels.

References

1. K Rabensteiner, "Advanced tunnel surveying and monitoring", *Felsbau*, vol. 14, no. 2, pp. 98-102, 1996.
2. N de Battista, M Elshafie, K Soga, M Williamson, G Hazelden and Y S Hsu, "Strain monitoring using embedded distributed fibre optic sensors in a sprayed concrete tunnel lining during the excavation of cross-passages", Proceedings of 7th International Conference on Structural Health Monitoring of Intelligent Infrastructure, Torino, Italy, 1-3 July, 10 p., 2015.
3. C Monsberger, H Woschitz, W Lienhart, V Račanský and M Hayden, "Performance assessment of geotechnical structural elements using distributed fiber optic sensing", Proceedings of SPIE 10168: Smart Structures and NDE, Portland (OR), USA, 25-29 March, pp. 101680Z1-12, 2017.
4. F Moser, W Lienhart, H Woschitz and H Schuller, "Long-term monitoring of reinforced earth structures using distributed fiber optic sensing" *Journal of civil structural health monitoring*, vol. 6, pp. 321-327, 2016.
5. M Wuilpart, Rayleigh scattering in optical fibers and applications to distributed measurements in *Advanced Fiber Optics: Concepts and Technology*, Luc Thévenaz (ed.), EPFL Press, Lausanne, Switzerland, 2011.
6. Luna Innovations Inc., Data Sheet: Optical Backscatter Reflectometer (Model OBR 4600), Ver. LTOBR4600 REV. 006 03/09/2018, 1 p, 2018.

7. S T Kreger, D K Gifford, M E Froggatt & B J Soller and M S Wolfe, "High resolution distributed strain or temperature measurements in single-and multi-mode fiber using swept-wavelength interferometry", Proceedings of Optical Fiber Sensors 2006, Cancun, Mexico, 23-27 October, ThE 42, 4 p, 2006.
8. Brugg Cables AG, Data Sheet: BRUsens strain V3. Vers. 2012/06/12 Rev. 02 TH, 1p, 2012.
9. Luna Innovations Inc., User Guide: Optical Backscatter Reflectometer Model OBR 4600, Ver. User Guide 5, OBR 4600 Software 3.6, 230 p., 2014.
10. H Woschitz, F Klug and W Lienhart, "Design and calibration of a fiber optic monitoring system for the determination of segment joint movements inside a hydro power dam", Journal of Lightwave Technology, vol. 33, no. 12, pp. 2652-2657, 2015.
11. M N Alahbabi, Y T Cho, and T P Newson, "Simultaneous temperature and strain measurement with combined spontaneous Raman and Brillouin scattering," Optical Letter, vol. 30, no. 11, pp. 1276-1278, 2005.
12. M R Henzinger, T Schachinger, W Lienhart, F Buchmayer, W Weilingner, R Stefaner, M Haberler-Weber, E M Haller, M Steiner, W Schubert, "Faseroptisch unterstützte Messmethoden zur Beobachtung von Gebirgsdruck", Geomechanics and Tunnelling, vol. 11, no. 3, 2018. (in print)
13. L Wagner, "Concept and realisation of a distributed fibre-optic sensing system for direct and continuous strain measurement in a shotcrete lining," Master's thesis, Institute of Rock Mechanics and Tunnelling, Graz University of Technology, Austria, 2017.
14. OeGG, Handbook – Geotechnical Monitoring in Conventional Tunnelling, OeGG – Austrian Society for Geomechanics, Salzburg, Austria, 2010.